

Designing a Hard Disk Drive Kinetic Air Particle Detachment System Using Finite Element Analysis

Nualpun Jai-Nagam^a and Kiatfa Tangchaichit^{b,*}

Mechanical Engineering Department, Khon Kaen University, Thailand
E-mail: ^anualpun.j@kkumail.com, ^bkiatfa@kku.ac.th (Corresponding author)

Abstract. This study investigates the use of kinetic air nozzle jet based cleaning system to purge unwanted particulate contaminants from HSA (head stack assembly) prior to assembly of the HSA into a finished hard drive. Technical, economic and environmental challenges have caused cleaning process development to shift away from chemical cleaning towards dry cleaning, while ensuring high particle removal efficiencies, reduced material loss and other damage. Finite element analysis was used to study the detachment of deposited particles using turbulent air flows and then this numerical model was used to design a better cleaning system. Experimentation was performed to determine the effectiveness of system and specification parameter such as nozzle design, distance of nozzle to target, angle and pulse. Removal of the contaminants was measured using an optical particle counter (OPC) to quantify the number and types of particles by using digital image analysis. The results showed that an air particle purge cleaning process can perform well for surface cleaning. The particle removal efficiency of air cleaning and purging increases with elapsed time and it is correlated to critical set up parameters, such as pressure, velocity, pulse interval and cleaning duration. The optimal velocity was determined to ensure no mechanical damage to the HSA. The removal efficiency for submicron-sized contaminants was observed to be highly correlated to drag force. Successful development of this type of this system could provide significant benefits for improving the process of particle cleaning, which can result in higher product reliability.

Keywords: Air flow, particle, hard disk drive, particle counter, CFD, finite element.

1. Introduction

The areal density of magnetic hard disk drives (HDDs) has increased enormously due to market demand for higher capacity per drive. One of the main problems in hard disk manufacturing is contamination from unwanted particles. As areal density increases, the disk surface becomes increasingly sensitive to small sized particles. This paper is going to focus on the head stack assembly (HSA) which is a key component of the write-read mechanism inside a hard disk drive.

Particle contaminants may be deposited on HSA surfaces before assembly into the HDD. The properties of these particles may result in a reduction in quality. For example, a conductive particle less than 1 μm in size that adheres to a substrate in an integrated or on the surface may cause an electrical short. The physical damage to head and disk caused by particle contamination and it was verified that the damages were typically caused by particle interaction ranging from light deformation to very deep circumferential scratches [1]. Similarly stainless steel particle can be detected at assembly HDD process and experiment is performed to study screw bit speed [2].

Even when high-efficiency air filtration systems are installed in the factory, particle contaminants cannot be completely eliminated; therefore, effective surface cleaning methods are required. Various surface cleaning methods have already been developed and some of them are used industrially. These cleaning methods can be divided into the following two categories: (1) wet cleaning, and (2) dry cleaning.

Wet cleaning is known to be effective for removing fine particles even if the particle size is less than 0.1 μm . Chemical additives or irradiation by ultrasonic waves can also be used to enhance the cleaning efficiency. Although wet cleaning has been widely used in industry due to its high removal efficiency, it requires a drying process after cleaning and results in the processing of a large amount of water. In addition, residues in the solution may deposit onto the surface after drying and cause recontamination. Among the limitations of wet processing are the high cost and purity requirements of cleaning agents and possible liquid residue causing adhesion of remaining particles.

Air based dry removal of surface contamination has become increasingly important in HDD cleaning applications. Dry surface cleaning is simple and environmentally friendly since a large amount of solution is not required. Micron-sized particulate contaminants that are adhering to surfaces were studied to remove by an air jet [3]. The effect of the surface material, contaminant particle size, and RH can be resulting on the removal efficiency [4]. The removal of submicron-sized particles was using consecutive pulsed air jets and analysed the removal efficiency taking into account the ratio of drag force to adhesion force. To improve the removal efficiency, electrostatic pre-charging and vibrating air jets were also investigated [5]. The experiment by releasing particle under a steady jet flow to avoid the transient effects was analysed [6]. Particle detachment from disk surfaces in disk drives has been studied. The conclusion is that detachment of sub-micron particles from the disk surface by using a slider air-bearing design is possible solution. They have also calculated the critical operating speed conditions for detachment of particles of various sizes and compositions [7].

Therefore, this paper will further study how to efficiently remove particle by using air nozzles to purge particles before HSAs are assembled into the final HDD. The goal is to meet the technical and economic challenges, which are leading cleaning process development away from chemistries, while also maintaining high particle removal efficiency, reduced material loss and other damage.

Although air cleaning methods are widely used on many types of components, they are seldom used on fragile parts such as HSAs. The design approach used finite element analysis to determine concept design and to develop optimal machine settings. The system is designed by same drive windage during operating.

2. Material and Methods

2.1 Fundamental of Air Flow Removal

In order to remove particle contamination from HSAs, the removal forces that act on the particles should be greater than the attractive adhesion forces. The most important adhesion forces are van der Waals forces and electrostatic forces. The strength of the van der Waals forces depends on the particle material as well as the particle size. Electrostatic forces depend, in addition to material properties, on the pH of the solution and can be attractive or repulsive. It is a longer range force than the van der Waals [8].

Mathematically, airflow pattern can be determined by a system of differential equations—conservation equations and turbulence equations, to determine the force acting on the particles, we will consider a discrete

particle traveling in a continuous fluid medium. The force acting on the particle that affects the particle acceleration is due to the difference in velocity between the particle and fluid, as well as the displacement of the fluid by the particle. The equation of motion for such a particle was derived [9].

$$m_p \frac{dU_p}{dt} = F_D + F_B + F_R + F_{VM} + F_P + F_{BA} \quad (1)$$

F_D is drag force acting on the particle, F_B is buoyancy force due to gravity, F_R is forces due to domain rotation, F_{VM} is virtual mass force and this term is very important when the displaced fluid mass exceeds the particle mass. F_P is pressure gradient force. F_{BA} is force deviation in flow pattern from a steady state. The subscript _p means particle and _F means fluid.

The aerodynamic drag force on a particle is proportional to the slip velocity, U_s , between the particle and the fluid velocity:

$$F_D = \frac{1}{2} C_D \rho_F A_F |U_s| U_s = \frac{1}{2} C_D \rho_F A_F |U_F - U_P| (U_F - U_P) \quad (2)$$

where C_D is the drag coefficient and A_F is the effective particle cross section. The drag coefficient C_D is introduced to account for experimental results on the viscous drag of a solid sphere.

The Reynolds number for a particle on a surface is given by [10].

$$R_e = \frac{\text{inertial forces}}{\text{viscous forces}} = \frac{\rho V L}{\mu} = \frac{V L}{\nu} \quad (3)$$

$$R_e = \frac{\rho V L}{\mu} = \frac{\left(1.225 \frac{\text{kg}}{\text{m}^3}\right) \times \left(25 \frac{\text{m}}{\text{s}}\right) \times \left(48 \times 10^{-3} \text{m}\right)}{1.81 \times 10^{-5} \frac{\text{kg}}{\text{m} \times \text{s}}} = 81200$$

Since the Re is more than 4000, then a commercial CFD solver with the k- ϵ turbulence model is used to determine the particle behavior of the system. Widely used of k- ϵ turbulence, one of example is to apply this k- ϵ turbulence in thermal convection and air flow velocity was adjusted and simulated in range m 5 to 20 m/s at the exhaust fan duct [11].

Table 1. Physical air properties.

Properties	Air
Density (kg/m ³)	1.225
Dynamic Viscosity (kg/m.s)	1.81E-5
Length of part (m)	48E-3
Velocity (m/s)	25

The CFD is using to calculate the velocity when the drive is operating, this is to get the reference velocity during drive operating and this number is going to be minimum velocity target to develop cleaning system by kinetic air flow.

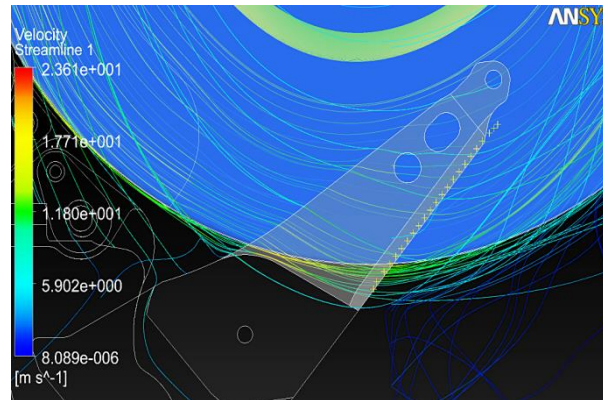


Fig. 1. Vector of vortex shedding of air flow and velocity max when drive operating @ 25 m/s.

Small particles are held by very strong surface forces which are a combination of physical attractions, chemical bonds, and mechanical stresses. This is referred to as adhesion force. It is therefore necessary to consider various means of removal [12].

The kinetic separation and the aerodynamic drag separation have been investigated by taking into account the forces acting on a particle adhering to a surface studied and particle removal was explained by the moments of the forces. [13-19]

There are three main forces that must be considered for particle removal: 1) Impact force caused by an airborne particle (F_c); 2) Drag force (F_d), and; 3) Adhesion force (F_a). Gravitational force can be neglected since the contaminants are very small. In Fig. 1, D_{p1} and D_{p2} are the diameters of the airborne particle and the particle adhering to the substrate, respectively, ϕ is the impact angle, θ is the contact angle based on elastic deformation, and M_t is the moment of force at the center of mass of the particle, which is caused by the shear flow. The balance of the moments of forces is represented by [20].

$$\{F_c \cos \phi (\sin \phi + \cos \theta) + F_d \cos \theta\} \frac{D_{p2}}{2} + M_t = \{F_c \sin \phi (\cos \phi + \sin \theta) + F_a \sin \theta\} \frac{D_{p2}}{2} \quad (4)$$

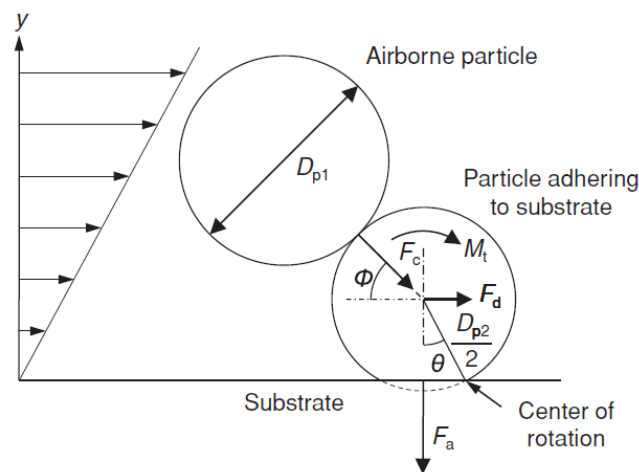
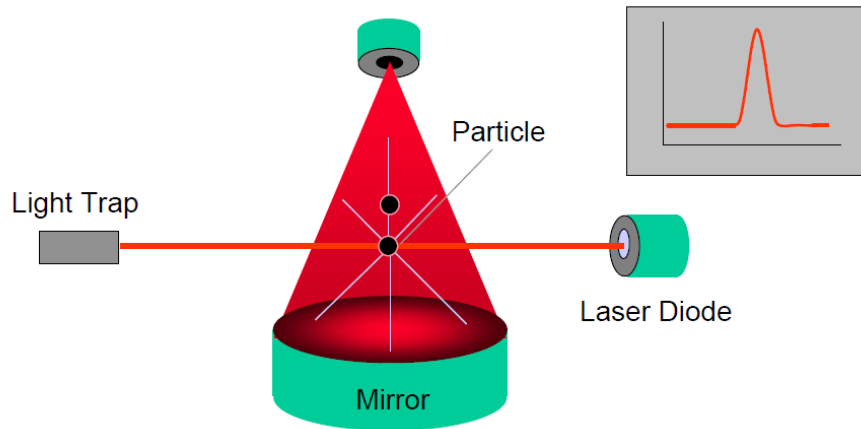


Fig. 2. Simple model of particle impact in shear flow field.

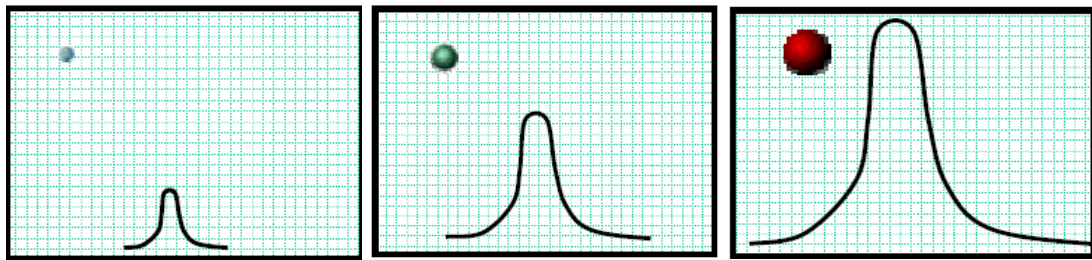
In this study, the removal of particulate contaminants adhering to a surface by air nozzle and vacuum particle out was experimentally investigated.

The particle removal surface was observed by using a combination of a high-speed microscope camera, SEM/EDX and OPC (Optical Particle Counting) equipment. The HDD industry currently uses this type of equipment for particle count monitoring [MET ONE Company]. This system is called Optical Particle Counting. This Optical Particle Counters (OPCs) employ mirrors and lenses to collect scattered light and focus this scattered light onto a photodetector. The photodetector then converts the scattered light into

electrical signals or “pulses”. Each pulse correlates to a particle size, and the instrument converts these pulses to numerical particle size data and the larger the particle is the larger the corresponding output pulse from the sensor which is illustrated in Fig. 3.



(a) Schematic of OPC system



(b) Particle sizing determination from optical particle count

Fig. 3. Principle of light scattering plot of optical particle counter equipment.

2.2. Experimental Procedures

This experiment is going to use the model of the hard disk drive that is currently available in the market as the tested parts.

The experiment procedure was conducted per the following steps as shown in Fig. 4:

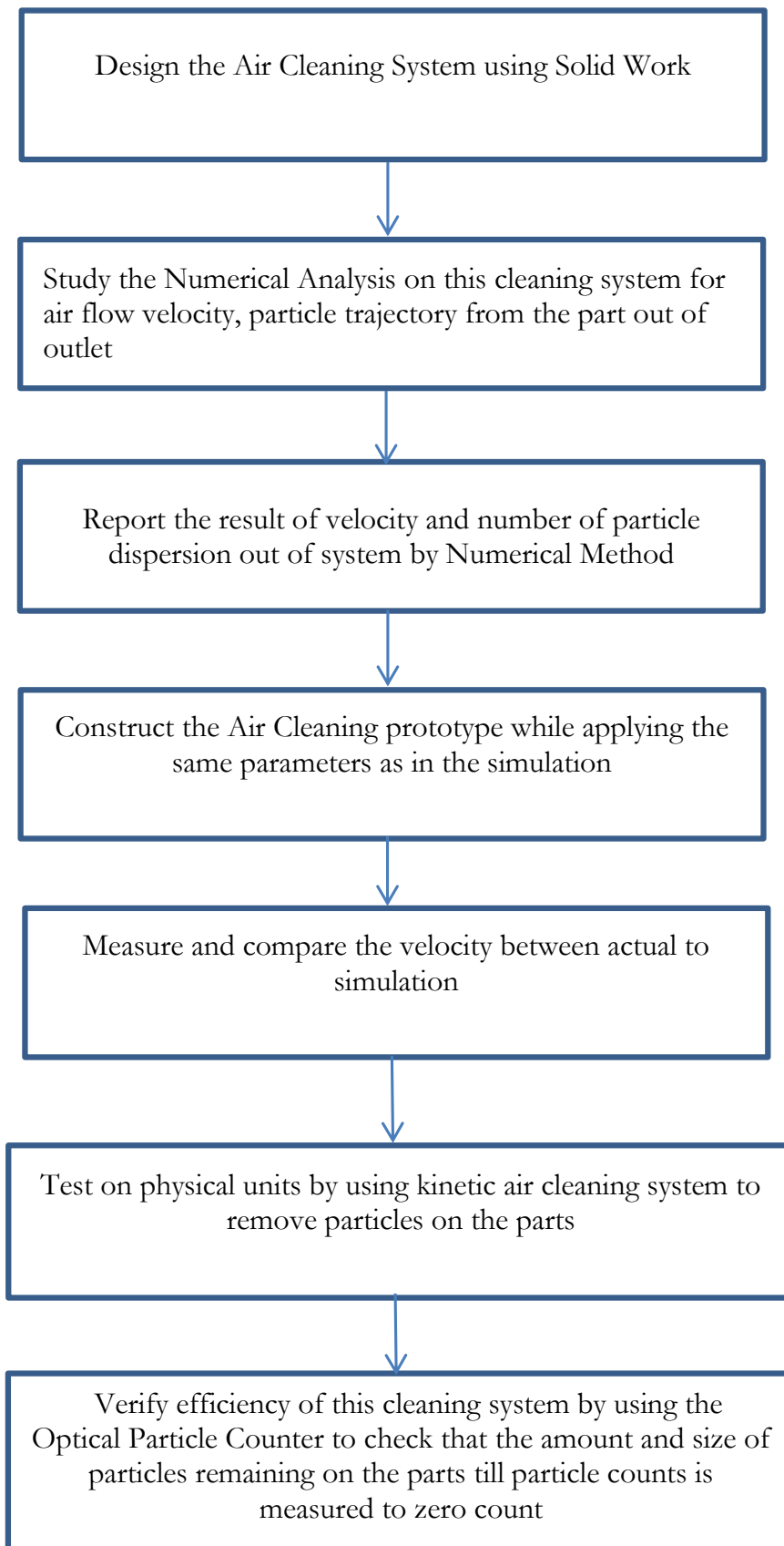


Fig. 4. Experiment analysis methodology.

The system will be tested the ability of an air stream from a nozzle to flow out extraneous particles from HSA surfaces as shown in Fig. 5. Following HSA assembly, multiple HSAs are packaged together, which are then sent in bulk to the HDD assembly line. A single HSA is contained in each “pocket” of the bulk packaging as illustrated in Fig. 6. Clean air fluid is injected into an inlet to release and remove particles.

The experiment will help determine the optimal recipe of air pressure, distance from nozzle to HSA, Nozzle Angle, and Pulse interval, which results in the best particle removal performance. The right combination of these variables should enhance the release of particles from components in the HSA surface into the purge fluid, which is then exhausted through an outlet.

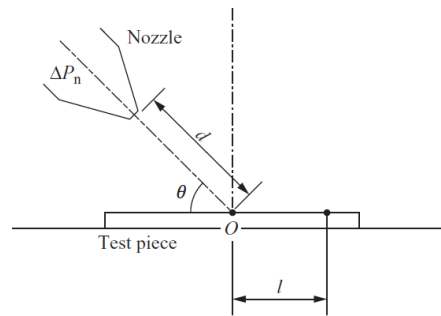


Fig. 5. Geometric parameters for arrangement of the nozzle and the surface.

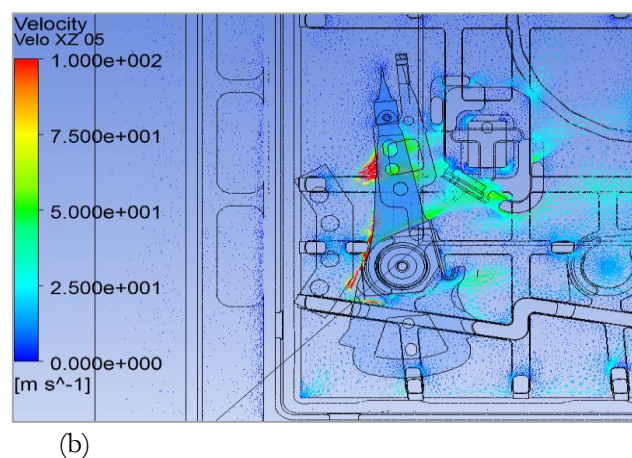
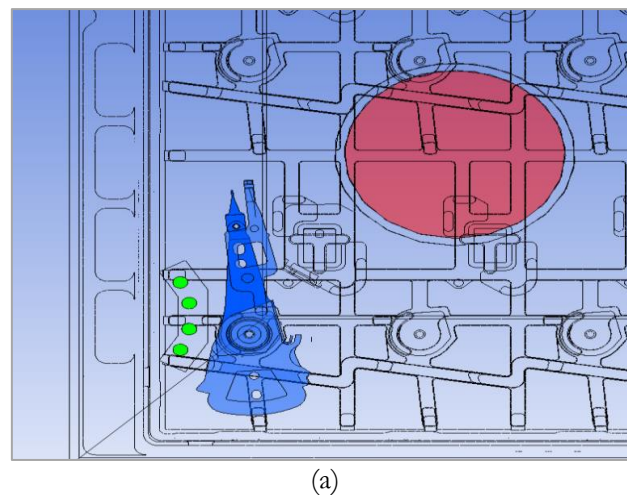


Fig. 6. (a) HSA in containing packaging; (b) HSA air cleaning CFD study.

2.3. The Setup Conditions for the CFD STUDY

2.3.1. Nozzle exit shape

Several type of nozzles are available in the market, this study is uses a commercially available rectangular nozzle as shown in Fig. 7.

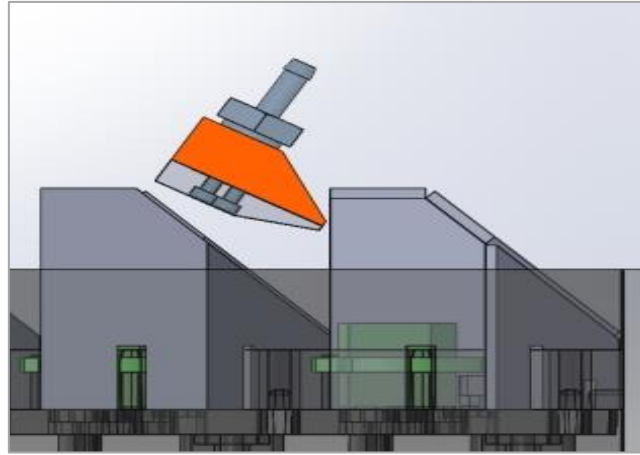


Fig. 7. Schematic view of the air jet nozzle.

2.3.2. Distance from nozzle to HSA

Determine the optimal distance between Nozzle and HSA in order that the air stream is strong enough to remove particles. The simulation in Fig. 6(b) showed that the result air velocity should be in the range of 25 m/s to 50 m/s

2.3.3. Impinging angle

In air jets used for cleaning, such as in air knives, the angle of the air jet should be between 30- 45 degrees to the surface to maximize cleaning efficiency. The optimized angle depends on many factors, two of the most important being the pressure delta, and the distance from the surface as illustration in Fig. 8.

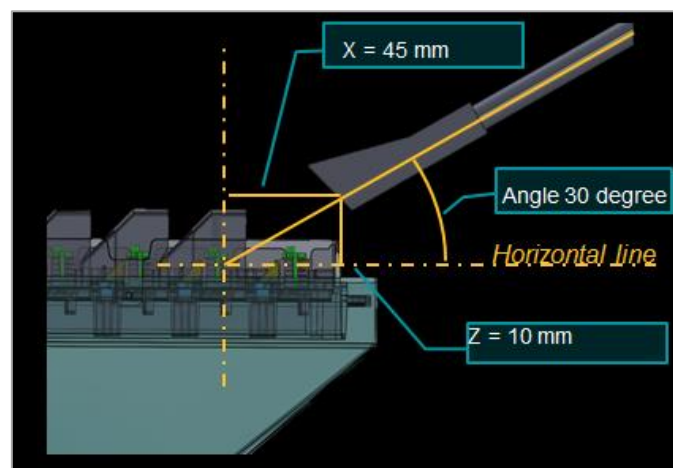


Fig. 8. Schematic view of the air nozzle angle and distance from test pieces.

2.3.4. Pulse interval

Otani et al. [21] found that the removal efficiency increased with increase in the number of pulsed jets. Ziskind et al. [22] also found that there is a marked enhancement of the removal efficiency at a certain frequency. However this study will focus on the pulse interval.

2.3.5 Air fin to control air flow direction

Since there are many HSAs, the amount of air pressure to gain most cleaning effectiveness required an air fin design as shown in Fig. 9 to help control the air flow stream. Key requirements of air fin design are to ensure that the direction and strength of the air flow stream are sufficient to effectively remove particles and keep them in the air stream without dispersing. Beside that the air fin should be able to move up to z direction so that air nozzle can move to another position.

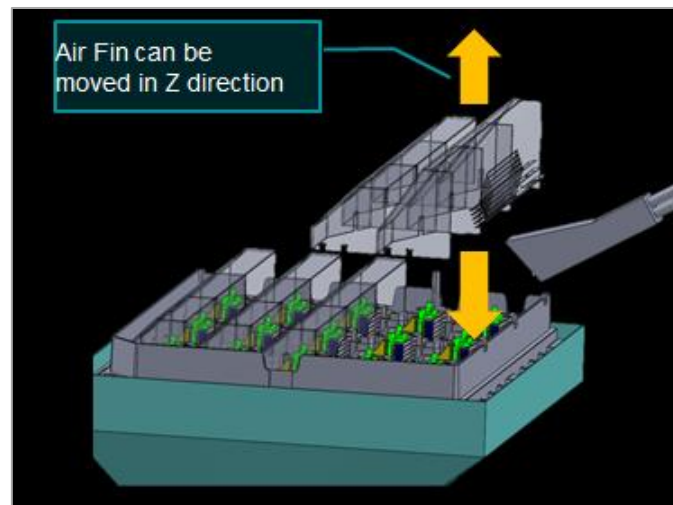


Fig. 9. Air fin to control air flow direction.

Table 2. Air cleaning setup specifications.

Parameter	Description
Air inlet pressure (psi)	30
Nozzle exit shape	Rectangle
Surface material	Stainless Steel
Particle diameter (μm)	0.3,1,5
Distance from nozzle(mm)	X= 45 , Z =10
Impinging angle ($^{\circ}$)	30
Duration of pulse (sec)	1
Pulse interval (sec)	3
Cleaning duration / cycle (sec)	6
Outlet pressure (psi)	10

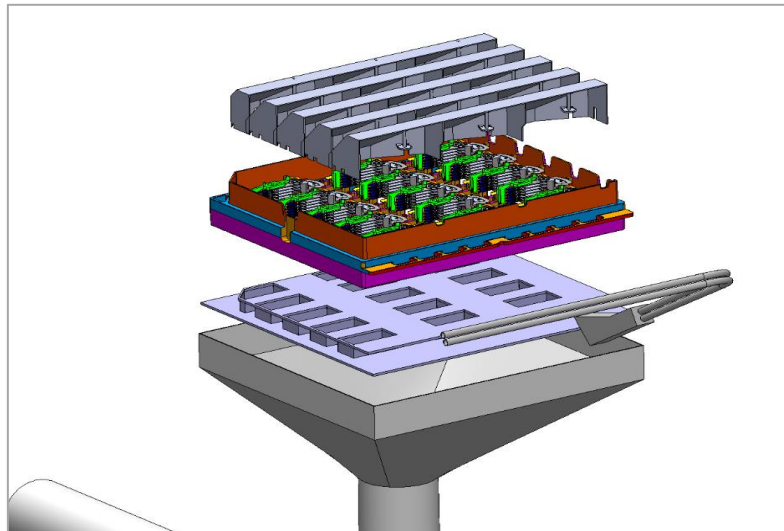


Fig. 10. Schematic view of overall system.

2.4. Mesh and Element

This air cleaning system has been constructed using a basic airflow model and solid works to design the overall system as illustration in Fig. 10. This model included all of the setup specifications that is indicated in Table 2 such parameters as nozzle design, air flow impinging angle and pulse interval etc.

ANSYS simulation software, run on a system using a 64bit CPU, was used to perform this numerical analysis. The fluid model shown in Fig. 10 was constructed using a tetrahedral mesh model with 22.7 million elements and 4.3 million nodes. An example of the resulting mesh is shown in Fig. 11. This was the best model in terms of the quality of the results and computation time. The quality of the model was verified using factors such as skewness, which was a very low 0.0001%. Therefore this model was considered excellent, skewedness ranged between 0-0.25% is considered excellent result, and appropriate to use for continuing the analysis.

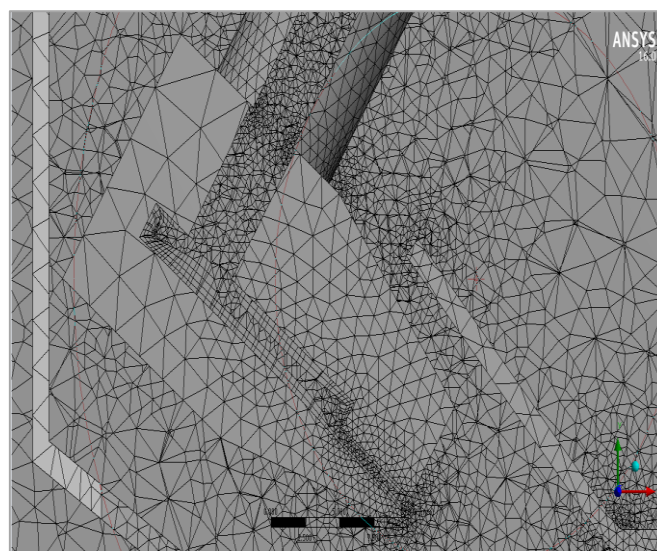


Fig. 11. Mesh model of air cleaning system at nozzle area.

Furthermore, the residual level which is the solution imbalances is verified to determine this numerical analysis converged in an acceptable manner to do further study. The residual of this model was set up at $1E-4$, this is considered sufficient for this model. With the RMS residuals at $1E-4$, the qualitative behaviour of the particle velocity, particle trajectory is clearly reported. We also analysed and compared the target to be

at 1E-5 and 1E-6. The difference in the velocity distribution between the resulting models that used residual levels of 1E-5 and 1E-6, was almost negligible because residuals were not reduced any farther. From this convergence condition the experimental and the model have an error lower than 0.1445%.

3. Result and Discussion

3.1. Pressure on Surface

Pressure at the impingement point was measured to directly determine the mass flowrate of the air jet. The pressures were measured under steady state conditions with flow temperatures of 25°C at the air nozzle. The pressure increases with the mass flow rate, and since the local pressure correlates with the mass flow rate of the jet flow, the local pressure can be used to evaluate the strength of the jet flow.

3.2. Air Flow Velocity

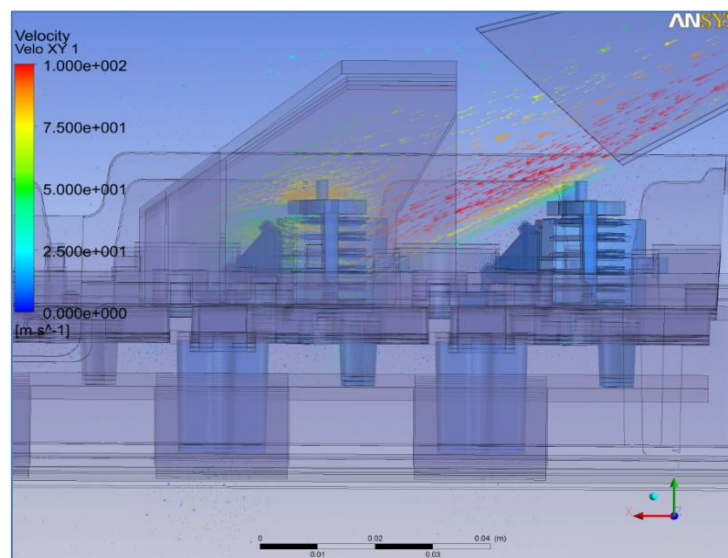
To evaluate the strength of the jet flow on the surface, the velocity has been measured at several areas to ensure that the final result of air flow velocity can meet the target 25 m/s, or higher, as shown in Fig. 1. This is to get the minimum force to remove the particles.

From the CFD model output, the velocity is a critical parameter that would result in drag force. The resulting velocity from the model indicates that it meets the requirement of being over 25 m/s and the air flow from the model shows that it has well streamline around surface of HSA that mean the air flow can be clean out particle whole HSA area that contour of velocity from model has reported in Fig. 12.

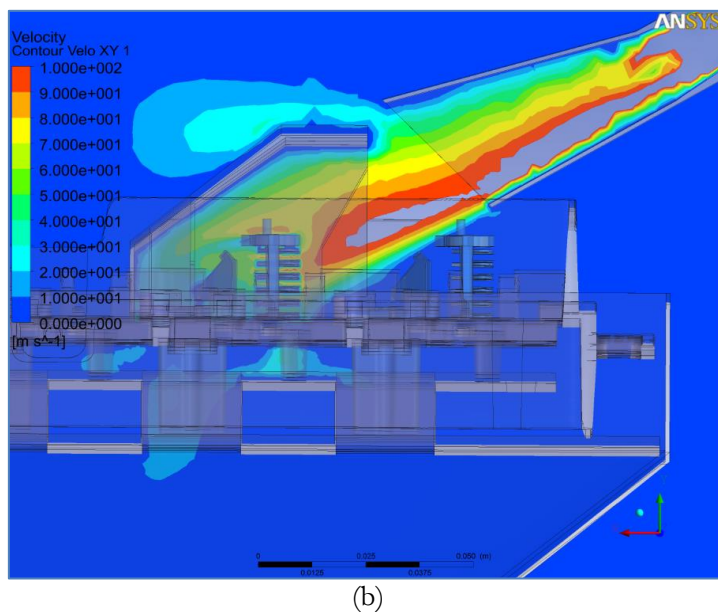
After that the prototype was built to test this particle removal effectiveness, the velocity was one of the parameters used to verify the model. The measurement of the velocity of the system showed that the deviation from simulation was within the acceptable range of less than 10%.

Table 3. The velocity from simulation and mock up prototype comparison.

Position	Velocity (m/s)		Deviation in Percentage
	Minimum velocity from Simulation	Actual measurement using the velocity probe	
Arm tip	30.6	28.5	7%
Arm Root	26.9	25	7%
Bearing	26.7	25.5	4%
Coil	25.2	25	1%



(a)



(b)

Fig. 12. (a) Velocity and air streamline from FEM; (b) Velocity and air flow contour.

The finite element analysis also studied and simulated by releasing of 5,000 stainless steel particles to the system to see if such particles could be removed from the system. The simulated particle trajectory is shown in Fig. 13.

It can be seen that most of the particles in every area were purged quickly through the outlet pipe. To confirm these results, the simulation was repeated 30 times with a total of 150,000 released particles, followed by conducting a count of the number of unpurged particles. The number of particles can be purged out from the system is approximately 95% which is calculated from the particle that count from the mass flow rate at outlet position which is 143550 in total counts.

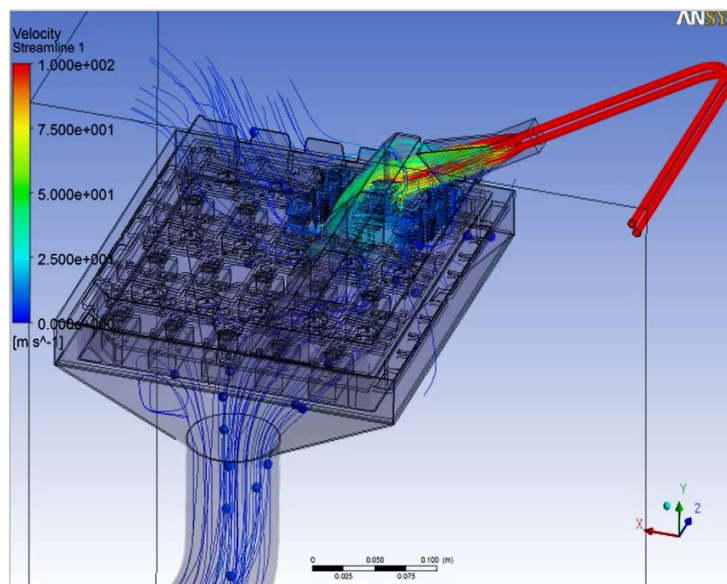


Fig. 13. Trace of released particle.

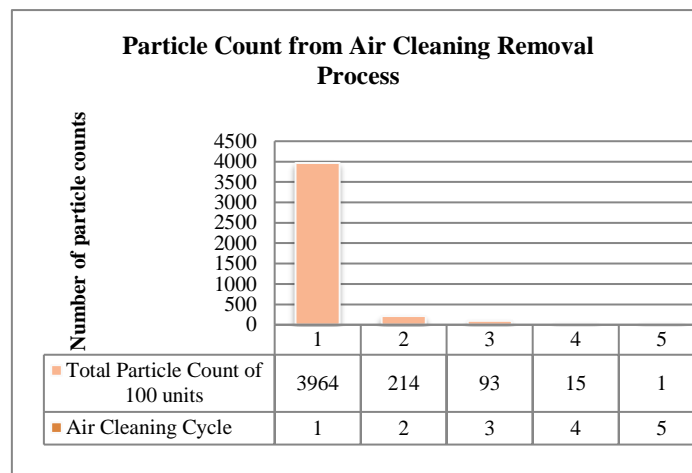
3.3. Particle Count Study with Prototype Set up

The efficiency of the removal of particulate contaminants was determined using a commercially available Optical Particle Counter (OPC-METONE). This Optical Particle Counters (OPCs) employ mirrors and lenses to collect scattered light and focus this scattered light onto a photodetector. The photodetector then converts the scattered light into electrical signals or “pulses”. Each pulse correlates to a particle size, and the instrument converts these pulses to numerical particle size data and the larger the particle is the larger the corresponding output pulse from the sensor.

The group of parts was cleaned by kinetic air cleaning and the particles were purged out from outlet. The Optical Particle Counter that was installed as part of this air cleaning system was used to measure the particle counts that were removed by the air cleaning. The experiment flow is shown how to clean HSA and then later measure the particle count and size is shown in Fig. 14.

Table 4 shows the particles removal counts from each cycle in the cleaning scheme. The results showed that the first cycle had the highest cleaning effectiveness. The HSA sample size was 100 units, with the 3964 total particles cleaned out in the first cycle. Further cycles were performed until the OPC detected no more particles being purged from the parts. In summary, total particle from OPCs can count total 4287 particle and the 1st cleaning could remove out 3964 particles or 92% removal efficiency.

Table 4. Particle count from air cleaning removal process.



3.4. Time-Dependent Particle Removal Efficiency

Table 4 indicates that the cleaning setup used in the study is able to clean particle effectively. In order get the maximum effectiveness; the number of cleaning cycles was extended to be 5 times in total, each cycle being 6 seconds in duration. The number of particles removed in the first cycle was 92% (3964/4287) of the total particles removed. The calculation is weighted by the total counts of particle of this group sample of 4287 particle counts, as obtained from the OPC. This is similar to the simulation, which showed that approximately 95% of the particles could be purged using the air jet method.

The OPC is also reported the size of detected particle as illustration in Fig. 3. Figure 15 shows that the removal rate for 0.3 μ m particles is much higher than that for 0.5 μ m, 1 μ m and 5 μ m particles. This can be interpreted that the aerodynamic drag force acting on the contaminants can be overcome by impact force from pressure and the pulse of pressure can enhance removal rate that are key parameters of kinetic air cleaning system.

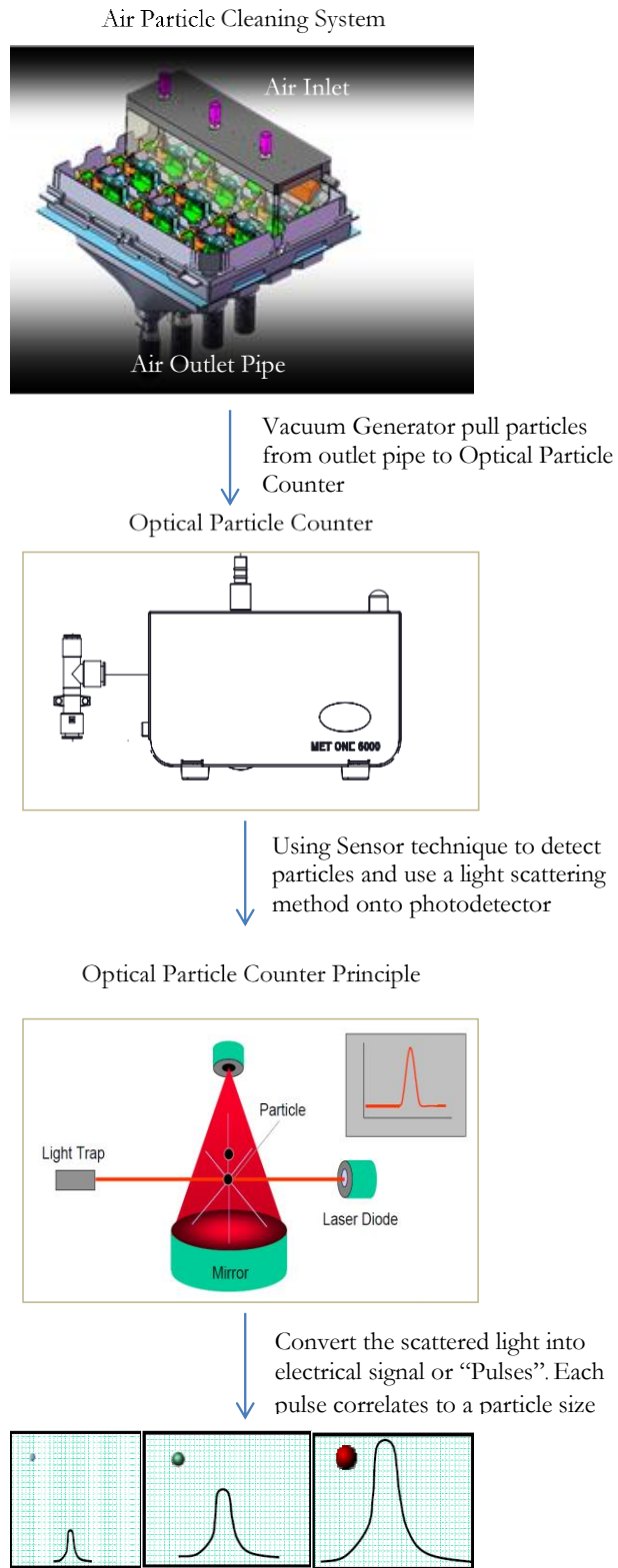


Fig. 14. Experiment Flow how to measure particle count and size.

Table 5. % Particle Removal Effectiveness over time.

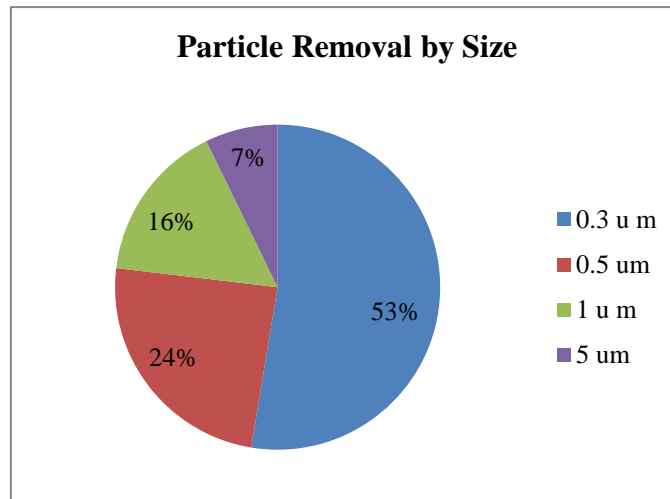
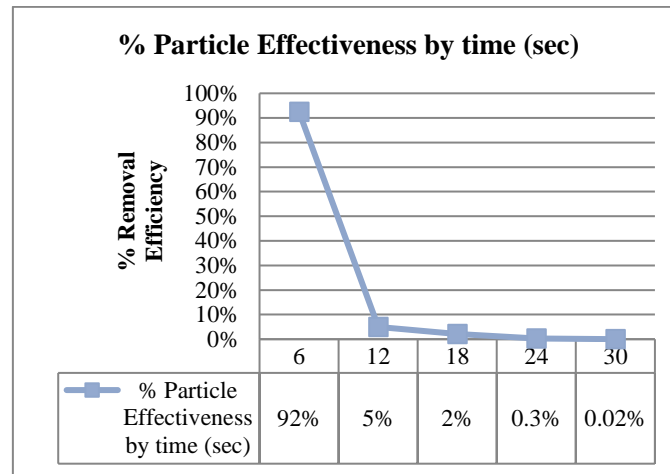


Fig. 15. Particle removal rate by size.

Further analysis was done on the particles that were purged by this air cleaning system, in order to understand the benefits of this next step of process improvement and particle contamination reduction. The particles captured in the OPC filter were examined by SEM/EDX analysis in order to identify the type of particle and % of total particle count. This data is shown in Fig. 15. Further interpretation of this data can help to understand which type of particles from this air cleaning system is most effective at removing. This will help to minimize the particles that would be harmful to HDD. From Fig. 16, Stainless Steel particles are top Pareto that will need to further improvement.

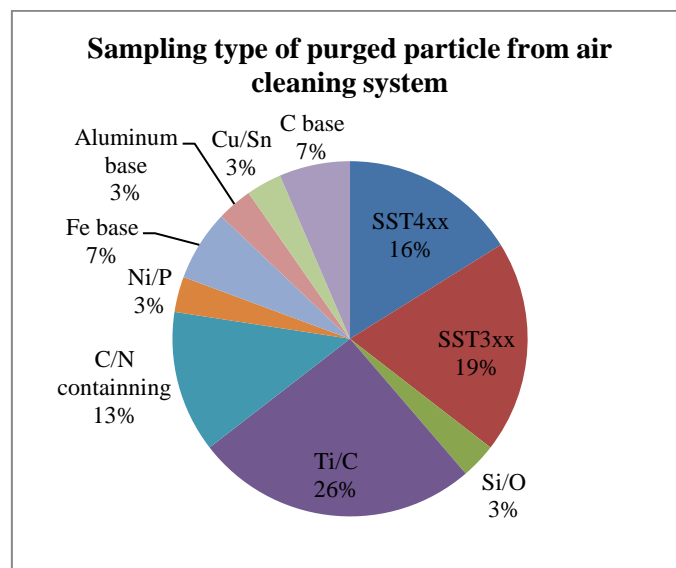


Fig. 16. Types of particle that were cleaned from the surface.

4. Conclusion

Finite Element Analysis of turbulent air flows was used to design a new particle contaminant removal system that uses kinetic air flow to purge out particles from disk drive HSAs. The removal process was simulated during the design calculations and the various parameters were modelled to understand how to maximize the removal of particles without damaging the HSA. An experimental prototype was built and the particle removal process was documented over time in order to determine the particle removal efficiency. Finally, an analysis was performed to determine the quantity and type of particles removed. Following are the main observations and conclusions:

- 1) Some of the key variables for detachment of deposited particles in turbulent air flows are nozzle exit shape design, air fin to control air streamline, target height from nozzle to parts, Impinging Angle, Pulse interval, Pulse duration and cleaning cycle time that to get final pressure and velocity to remove the particle out of HSA Surface.
- 2) Effective coverage of the surface cleaning area and particle removal efficiency depends on the strength of the air nozzle jet, which was evaluated by the input pressure and velocity on the surface. To remove submicron-sized contaminants, an optimum pressure or air flow velocity and air flow streamline is required that will detach particles without damaging the fragile HSA. In addition the air velocity should be stable and similar to, or higher than normal drive operating conditions in order to get a similar impact force.
- 3) The particle removal efficiency of air cleaning and purge particle increases with elapsed time. However the length of this time should be considered in case it increases the manufacturing cycle time, since this could reduce output. The effectiveness of the first cycle of cleaning was up to 92% removal of the submicron-sized particles, with the removal efficiency falling off significantly in subsequent cleaning cycles. Therefore, prolonged cleaning cycles are unlikely to improve removal efficiency significantly.

In conclusion, this particle removal system has shown that it could provide significant benefits in terms of process improvement to minimize particle contamination. Overall cycle time can potentially be improved. This air cleaning system can have lower environmental impact if a shorter air-based cleaning process can replace lengthy and more costly chemical washing and drying of parts. Also it can capture and identify types of particles removed, the new system can be a good tool to help with root cause identification of how these particles are introduced into the manufacturing process to begin with.

Reference

- [1] L. Zhang, R. Koka, Y. Yuen, and E. Lam, "Particle induced damage on heads and discs due to fine Particles of different materials," *IEEE Trans. Magn.*, vol. 35, no. 2, pp. 927–932, 1999.
- [2] S. Laksanasittiphan, K. Tuchinda, A. Manonukul, and S. Suranuntchai, "Experimental study of particles induced by screw tightening process for hard disc drive assembly: Effects of 'bit' speed," *Engineering Journal (Eng. J.)*, vol. 22, no. 1, pp. 65–76, Jan. 2018.
- [3] H. Masuda, K. Gotoh, H. Fukada, and Y. Banba, "The removal of particles from flat surfaces using a high-speed air jet," *Adv. Powder Technol.*, vol. 5, pp. 205–217, 1994.
- [4] K. Gotoh, K. Karube, H. Masuda, and Y. Banba, "High-efficiency removal of fine particles deposited on a solid surface," *Adv. Powder Technol.*, vol. 7, pp. 219–232, 1996.
- [5] Y. Otani, N. Namiki, and H. Emi, "Removal of fine particles from smooth flat surfaces by consecutive pulse air jets," *Aerosol Sci. Technol.*, vol. 23, pp. 665–673, 1995.
- [6] G. T. Smedley, D. J. Phares, and R. C. Flagan, "Entrainment of fine particles from surfaces by gas jets impinging at normal incidence," *Exp. Fluids*, vol. 26, pp. 324–334, 1999.
- [7] C. Tsai, Y. David, H. Pui, Y. Benjamin, and H. Liu, "Particle detachment from disk surface of computer drives," *J. Aerosol Sci.*, vol. 22, no. 6, pp. 737–746, 1991.
- [8] R. Kohli and K. L. Mittal, "Cleaning using high-speed impinging jet," *Developments in Surface Contamination and Cleaning*, vol. 1, 1st ed. San Diego: William Andrew Publishing, 2016, ch. 15, pp. 667–693.
- [9] ANSYS, "Particle transport theory," in *ANSYS CFX-Solver Theory Guide*, 13th ed. ANSYS, Inc., 2010. ch. 6.
- [10] Wikipedia. (2017). *Reynolds number*. [Online]. Available: https://en.wikipedia.org/wiki/Reynolds_number [Accessed: 22 February 2017]
- [11] C. Suvanjumrat, "Implementation and validation of OpenFOAM for thermal convection of airflow," *Engineering Journal (Eng. J.)*, vol. 21, no. 5, pp. 225–241, Sep. 2017.
- [12] N. Tippayawong and I. Preechawuttipong, "Analysis of microparticle resuspension in turbulent flows with horizontally vibrating surface," *Australian Journal of Basic and Applied Sciences*, vol. 5, no. 7, pp. 356–363, 2011.
- [13] Y. Kousaka, K. Okuyama, and Y. Endo, "Re-entrainment of small aggregate particles from a plane surface by air stream," *J. Chem. Eng. Jpn.*, vol. 13, pp. 143–147, 1980.
- [14] H.-C. Wang, "Effects of inceptive motion on particle detachment from surfaces," *Aerosol Sci. Technol.*, vol. 13, pp. 386–393, 1990.
- [15] C. J. Tsai, D. Y. H. Pui, and B. Y. H. Liu, "Particle detachment from disk surfaces of computer disk drives," *J. Aerosol Sci.*, vol. 22, pp. 737–746, 1991.
- [16] S. Matsusaka and H. Masuda, "Particle reentrainment from a fine powder layer in a turbulent air," *Aerosol Sci. Technol.*, vol. 24, pp. 69–84, 1996.
- [17] H. Masuda, K. Gotoh, H. Fukada, and Y. Banba, "The removal of particles from flat surfaces using a high-speed air jet," *Adv. Powder Technol.*, vol. 5, pp. 205–217, 1994.
- [18] I. Adhiwidjaja, S. Matsusaka, H. Tanaka, and H. Masuda, "Simultaneous phenomenon of particle deposition and reentrainment: Effects of surface roughness on deposition layer of striped pattern," *Aerosol Sci. Technol.*, vol. 33, pp. 323–333, 2000.
- [19] W. Theerachaisupakij, S. Matsusaka, Y. Akashi, and H. Masuda, "Reentrainment of deposited particles by drag and aerosol collision," *J. Aerosol Sci.*, vol. 34, pp. 261–274, 2003.
- [20] Y. Liu, H. Maruyama, and S. Matsusaka. "Effect of particle impact on surface cleaning using dry ice jet," *Aerosol. Sci. Technol.*, vol. 45, pp. 1519–1527, 2011.
- [21] Y. Otani, N. Namiki, and H. Emi, "Removal of fine particles from smooth flat surfaces by consecutive pulse air jets," *Aerosol. Sci. Technol.*, vol. 23, pp. 665, 1996.
- [22] G. Ziskind, L. P. Yarin, S. Peles, and C. Gutfinger, "Experimental investigation of particle removal from surfaces by pulsed air jet," *Aerosol. Sci. Technol.*, vol. 36, pp. 652, 2002.
- [23] ANSYS, *ANSYS CFX-Solver Theory Guide*, 13th ed. ANSYS, Inc., 2010.